

# On the tuning of a hybrid observer for multiple frequency estimation

D. Carnevale and S. Galeani

**Abstract**—An adaptation algorithm for the parameters selection of the multiple frequency hybrid observer in [1] is proposed. The algorithm is tailored for numerical implementation and is aimed to retrieve, exploiting a suitable amount of past data, the number of frequencies of a signal and the observer gains to improve the exponential convergence to zero of the frequencies estimation error, even in case of noisy measurements.

## I. INTRODUCTION

The problem of finding the unknown angular frequencies  $\omega_i$ 's of the signal

$$y(t) = \sum_{i=1}^n E_i \sin(\omega_i t + \phi_i), \quad (1)$$

where also  $E_i$ 's and  $\phi_i$ 's are unknown, has been extensively addressed using classical Fourier analysis of batch data [2], on-line methods based on notch filters [3] and Kalman filters [4], adaptive schemes [5] and adaptive identifiers [6], [7], [8], filtered transformations [9], Immersion and Invariance techniques [10], and hybrid systems [1] just to name a few. With respect to the previous work, we further assume that the number of frequencies  $n$  of the signal (1) is not known, as in [11] and [12].

We propose an algorithm to estimate  $n$  and select the signal sampling time and the gains of the observer in [1] to provide an auto-tuned hybrid observer with improved performances. The selection of the gains in [1] (as well as in [10]) are crucial to obtain satisfactory performances and, as it will be pointed out in Section III, they depend on the value of the  $\omega$ 's and the sampling time  $T$  of the signal (1). More specifically, the observer in [1] requires the selection of the sampling time  $T$  to collect a given amount of samples of (1) which are processed to obtain the estimates of the  $\omega$ 's. Via numerical simulations the exponential convergence of the estimation error  $\omega - \hat{\omega}$  to zero has been seen to sensibly depend on the selection of  $T$ , that might be chosen in the wrong way up to to prevent convergence of the estimates (see Lemma 1). Then, we want to provide the hybrid observer in [1] with an algorithm that, processing a batch of past data, retrieves on-line the correct value of  $n$  and “best”  $T$ . In the companion paper [13] the techniques of this paper, combined with hybrid observer [1], are exploited to solve the problem of asymptotic regulation of linear systems in case of disturbances (references) generated by neutrally

stable linear systems of unknown dimension and parameters.

The paper is organized as follows: in Section II we recall the hybrid observer presented in [1] followed by the proposed approach which is motivated theoretically and numerically in Section III, where also the main algorithms are provided. Numerical simulations to show the effectiveness of the method are given in Section IV and conclusions are drawn in Section V.

## II. BACKGROUND

The signal (1) can be seen as the output  $y(t) = Cx(t)$ ,  $x \in \mathbb{R}^{2n}$ ,  $C = [0, 1, 0, 1, 0, \dots, 1]$ , of the linear, time-invariant system described by

$$\dot{x} = Ax = \text{diag} \left\{ \begin{bmatrix} 0 & \omega_i \\ -\omega_i & 0 \end{bmatrix} \right\} x, \quad i = 1, \dots, n, \quad (2)$$

with unknown initial condition  $x(t_0)$  and  $\omega_i$ 's. The method proposed in Section III exploits samples of (1) with re-sampling sampling time  $T$  to estimate the  $\omega$ 's. We assume that the re-sampling time  $T$  is defined as a multiple of the hardware sampling time  $T_s$ , namely  $T = pT_s$ , for some  $p \in \mathbb{N}_{\geq 1}$ . Then we define the measurements vector

$$Y_k := \begin{bmatrix} y(t_{k-2n}) \\ \vdots \\ y(t_{k-2}) \\ y(t_{k-1}) \end{bmatrix} = Ox(t_{k-2n}), \quad (3)$$

where  $t_k = kT$ , i.e.  $y(t_k) = y(kpT_s)$ , and

$$O := \begin{bmatrix} C \\ CA_D \\ \vdots \\ CA_D^{2n-1} \end{bmatrix}, \quad A_D := e^{AT}. \quad (4)$$

The characteristic polynomial of  $A_D$  is

$$p_{A_D}(\lambda) = \prod_{i=1}^n (\lambda^2 - 2 \cos(\omega_i T) \lambda + 1) \\ = \lambda^{2n} + a_{2n-1} \lambda^{2n-1} + \dots + a_1 \lambda + 1, \quad (5)$$

with symmetric coefficients, i.e. such that  $a_{2n-h} = a_h$ ,  $h = 1, \dots, n-1$ . The coefficients  $a_i$  of  $p_{A_D}(\lambda)$  can be compactly expressed as

$$a := \begin{bmatrix} 1 \\ a_1 \\ a_2 \\ \vdots \\ a_{2n-2} \\ a_{2n-1} \end{bmatrix} = \begin{bmatrix} 1 & 0 \\ 0 & S \end{bmatrix} \begin{bmatrix} 1 \\ a_1 \\ a_2 \\ \vdots \\ a_{n-1} \\ a_n \end{bmatrix} = \hat{S} \begin{bmatrix} 1 \\ a_c \end{bmatrix} \quad (6)$$

D. Carnevale and S. Galeani are with Dipartimento di Informatica, Sistemi e Produzione (DISP), Università di Roma “Tor Vergata”, 00133 Roma, Italy. E-mails: [carnevale, galeani]@disp.uniroma2.it

Supported in part by ASI, ENEA-Euratom and PRIN.

where  $S_i$  is the  $i$ -th row of  $S \in \mathbb{R}^{2n-1 \times n}$  and the matrices  $S$ ,  $\hat{S}$  and the coefficient vector  $a_c$  are defined according to

$$S_i := \begin{cases} 1 & \text{if } i = j \text{ or } 2n - i = j, \\ 0 & \text{otherwise,} \end{cases} \quad (7a)$$

$$\hat{S} = \begin{bmatrix} 1 & 0 \\ 0 & S \end{bmatrix}, \quad (7b)$$

$$a_{c,i} = a_i = f_i(\omega), \quad i = 1, \dots, n, \quad (7c)$$

where  $f_i(\omega) = \sum (-2)^i \mathcal{Q}_j^i(\omega)$  is the sum of the  $\binom{n}{i}$  monomials  $\mathcal{Q}_j^i(\omega)$ ,  $j = 1, \dots, \binom{n}{i}$ , with  $\mathcal{Q}_j^i(\omega)$  obtained as the product of the elements of the  $j$ -th combination without repetition of  $i$  elements of the set  $\{\cos(\omega_1 T), \dots, \cos(\omega_n T)\}$ . Equivalently, the  $f_i(\omega)$  corresponds to the coefficients of the characteristic polynomial of  $A_D$  in (5) for  $i = 1, \dots, n$ . The above definitions allow to write

$$y(t_k) = -Y_k' a = -Y_k' \begin{bmatrix} 1 & 0 \\ 0 & S \end{bmatrix} \begin{bmatrix} 1 \\ a_c' \end{bmatrix}, \quad (8)$$

and

$$Y_{k+1} = \begin{bmatrix} y(t_{k-4n+1}) & \cdots & y(t_{k-2n}) \\ \vdots & & \vdots \\ y(t_{k-2n-1}) & \cdots & y(t_{k-2}) \\ y(t_{k-2n}) & \cdots & y(t_{k-1}) \end{bmatrix} a = -\bar{Y}_k a. \quad (9)$$

It can be easily proven, by observability of the system (2), that  $\text{rank}(\bar{Y}_k) = 2n$  for almost all  $T > 0$ , i.e.  $\bar{Y}_k$  is full rank. Then, the vector  $a$  can be readily evaluated by

$$a = -\bar{Y}_k^{-1} Y_{k+1}, \quad (10)$$

collecting the first  $4n$  data to build the matrix  $\bar{Y}_k$ . This yield the true values of the parameters  $a_i$  in finite time.

*Remark 1:* The  $\omega_i$ 's can be obtained from the  $a_i$ 's finding the zeros  $\zeta_i \pm j\sqrt{1 - \zeta_i^2} \in (-1, 1)$  of the  $2n$  order polynomial  $\Pi_{i=1}^n (\lambda^2 - 2\zeta_i \lambda + 1)$  with  $\zeta_i = \cos(\omega_i T)$  and, as shown in Section III, with  $0 < \omega_i T < \pi$  so that  $\omega = \arccos(\zeta_i)/T$ . Namely, it is sufficient to run a root finding algorithm on the polynomial (5) with  $\lambda = e^{j\alpha}$  and  $\alpha \in (0, 2\pi)$ .

To render this method less sensitive to measurement noise, it is possible to consider more than  $2n$  samples  $y(t_k)$  piled in  $\bar{Y}_k$  exploiting pseudo-inverse to get estimates of  $a$  minimizing the mean squared error.

To obtain the vector  $a_c$  directly from the measures  $Y_k$  it is possible to define  $\bar{Y}_k^c$  as

$$\bar{Y}_k = [Y_{k-2n-1}, Y_{k-2n}, \dots, Y_k] \triangleq [Y_{k-2n-1}, \bar{Y}_k^c], \quad (11)$$

yielding

$$a_c = - (S' \bar{Y}_k^c \bar{Y}_k^c S)^{-1} S' \bar{Y}_k^c (Y_{k+1} + Y_{k-2n-1}). \quad (12)$$

It is important to note that the numerical invertibility of the matrix  $\bar{Y}_k$  is sensitive on the sampling time  $T$ . In fact, if  $T$  is too small with respect to the period  $T_i$  of the sinusoids  $\bar{Y}_k$  is ill-conditioned.

To briefly recall the hybrid observer  $\mathcal{H}$  in [1] for the estimation  $a_c$  define

$$A_0 = \begin{bmatrix} 0 & 1 & 0 & \cdots & 0 \\ 0 & 0 & 1 & \ddots & \vdots \\ \vdots & & & \ddots & 0 \\ 0 & \cdots & \cdots & 0 & 1 \\ 0 & \cdots & \cdots & \cdots & 0 \end{bmatrix}, \quad B_0 = \begin{bmatrix} 0 \\ \vdots \\ \vdots \\ 0 \\ 1 \end{bmatrix}, \quad (13)$$

with  $A_0 \in \mathbb{R}^{2n \times 2n}$  and  $B_0 \in \mathbb{R}^{2n}$ . Then the flow and jump maps of  $\mathcal{H}$  with state

$$\xi = [\hat{a}_c' \quad \zeta' \quad \chi \quad \tau]' \in \mathcal{O}, \quad (14a)$$

where  $\hat{a}_c \in \mathbb{R}^n$ ,  $\zeta \in \mathbb{R}^{2n}$ ,  $\chi \in \mathbb{R}$ ,  $\tau \in \mathbb{R}$ , are

$$\left. \begin{array}{l} \dot{\hat{a}}_c = -\gamma \hat{S}' \zeta e, \\ \dot{\zeta} = 0, \\ \dot{\chi} = 0, \\ \dot{\tau} = 1, \end{array} \right\} \text{if } \xi \in \mathcal{C}, \quad (14b)$$

$$\left. \begin{array}{l} \hat{a}_c^+ = \hat{a}_c, \\ \zeta^+ = A_0 \zeta + B_0 \chi, \\ \chi^+ = y, \\ \tau^+ = 0, \end{array} \right\} \text{if } \xi \in \mathcal{D}, \quad (14c)$$

where  $\hat{S}' = [0, S'] \in \mathbb{R}^{n \times 2n}$ ,  $\gamma > 0$  is the observer gain, and the error  $e$  is given by

$$e(t, k) = y(t_k) + \zeta(t, k)' \hat{a} = y(t_k) + Y_k' \hat{S} [1, \hat{a}_c(t, k)]'.$$

Note that hybrid time domains are considered (see [14]), meaning that each variable above is expressed as a function of  $(t, k)$ , where  $t$  is the flow time and  $k$  counts the jumps. The flow set  $\mathcal{C}$  and the jump set  $\mathcal{D}$  are defined as

$$\mathcal{C} \triangleq \{\xi \in \mathcal{O} : \tau \in [0, T]\}, \quad (14d)$$

$$\mathcal{D} \triangleq \{\xi \in \mathcal{O} : \tau \geq T\}. \quad (14e)$$

$\zeta$  maintains the past  $2n$  values of the input  $y$ , i.e.  $Y_k = \zeta(t, k)$  whereas  $\chi(t, k) = y(t_k)$  for all  $t \in [t_k, t_{k+1})$ . Note that  $2n$  samples of  $y$  have to be fetched in  $\zeta(0, 0)$  before starting. By definition of jump and flow sets, the observer resets are triggered each sample time  $T$ . The hybrid formulation allows to easily take into account jumps at sampling and continuous dynamics between them. The flow map of  $\hat{a}_c$  has been selected to minimize the Lyapunov function  $V(t, k) = \|\tilde{a}_c(t, k)\|^2 = \|a - \hat{a}_c(t, k)\|^2$  via a standard gradient algorithm which has been proved to yield exponential convergence of the estimation error  $\tilde{a}_c(t, k)$  to zero. The proof relies on the independence of the  $2n$  column vectors  $Y_k$ , i.e.  $\text{rank}(\bar{Y}_k) = 2n$ . The observer is then very simple and provides a continuous time estimate  $\hat{a}_c(t, k)$  which exhibits no jumps. In fact, each new sample of  $y$  is fetched in the  $\zeta$  whereas the oldest one is discarded, and only the flow vector field of  $\hat{a}_c$  is changed. It follows a standard assumption necessary to estimate the  $a_i$ 's and recalled by Theorem in [1].

*Assumption 1:* The parameters of the signal (1) satisfy  $E_i \neq 0$ ,  $0 < \omega_i < \pi/T_s$  and  $\omega_i \neq \omega_j$  for any  $i \neq j$  with  $(i, j) \in \{1, \dots, n\}$ .

*Theorem 1 ([1]):* Under the Assumption 1, the estimation error  $\tilde{a}_c(t, k) = \hat{a}_c(t, k) - a_c$  uniformly exponentially converges to zero as  $k$  goes to infinity.  $\square$

We remark again that the observer  $\mathcal{H}$  provides a continuous time estimate  $\hat{a}_c(t, k)$  which exhibits no jumps. To avoid the zero finding procedure discussed in Remark 1 it is possible to evaluate dynamically  $\omega$  substituting  $\hat{a}_c$  to  $\hat{\omega}$  in the state  $\chi$  of  $\mathcal{H}$  with the flow map

$$\dot{\hat{\omega}} = -\gamma \nabla f(\hat{\omega})' \hat{S}' \zeta e, \quad (15)$$

and jump map  $\hat{\omega}^+ = \hat{\omega}$ , with  $e = y(t_k) + \zeta' \hat{S} [1, f(\hat{\omega})]'$ . In this case, it can be proven that  $\text{rank}(\nabla f(\hat{\omega})) < 2n$  if and only if there exists  $j$  such that  $\omega_j = 0$  or  $\omega_j = \omega_i$  for some  $i \neq j$ , preventing the asymptotic convergence of the estimates. This issue can be avoided adding a “repulsive” term among the different  $\omega_i$ 's and the value zero in the jump or flow maps. However, even in simulation, numerical approximations and noise normally prevent this pathological behavior.

The parameters of the above observer are the number of frequencies  $n$ , the gain  $\gamma$ , and the sampling time  $T$ , i.e. the  $p \in \mathbb{N}_{\geq 1}$  such that  $T = pT_s$ . However, the sensitivity of the performance with respect to  $\gamma$  is negligible in comparison with the importance of  $n$  and  $T$ , the latter of which improves convergence performances if properly chosen.

### III. MAIN RESULT

To retrieve the number of frequencies  $n$  we propose to exploit the rank of the matrix  $\bar{Y}_k$  considering a re-sampling with different  $T$  on a moving window of input past data. To this aim, we evaluate on-line the minimum eigenvalue  $\lambda_{\min}(\bar{Y}_k' \bar{Y}_k)$  by re-sampling the past input data with increasing  $p = 1, 2, \dots$ ,  $T = pT_s$ . This choice is motivated directly by the proof of Theorem 1 that relies on the positive-definiteness of the matrix  $\bar{Y}_k' \bar{Y}_k$ , i.e. on the existence of a constant  $\delta > 0$  such that

$$\bar{Y}_k \bar{Y}_k' > \delta I,$$

with  $\delta = \lambda_{\min}(\bar{Y}_k' \bar{Y}_k)$ . Note that this selection speeds up the “slowest” converging error  $e_i = \omega_i - \hat{\omega}_i$ . Nevertheless there might be other values of  $T$  leading to faster transients. To start with, we notice that the hardware sampling time  $T_s$  limits the higher angular frequency that can be reconstructed to  $\omega_{\max} := \pi/T_s$  by Nyquist-Shannon’s Theorem.

*Lemma 1:* Assume that  $\omega_i < \omega_{max}$  for all  $i = 1, \dots, n$  and that  $x_0$  excites all the modes<sup>1</sup> of (2). Let  $\bar{Y}_k \in \mathbb{R}^{2\hat{n} \times 2\hat{n}}$  be obtained by the samples  $y(t_k)$  with sampling time  $T$ , then

- i)  $\text{rank}(\bar{Y}_k) = 2\hat{n}$  if  $\hat{n} \leq n$  and  $T < \pi / \max_i \{\omega_i\}$
- ii)  $\text{rank}(\bar{Y}_k) < 2\hat{n}$  if  $\hat{n} = n$  and  $T = \pi / \omega_i$  for  $i = 1, \dots, n$
- iii)  $\text{rank}(\bar{Y}_k) < 2\hat{n}$  if  $\hat{n} > n$  and  $T < \pi / \max_i \{\omega_i\}$ .

$\square$

The items of Lemma 1 suggest a test for identifying the correct  $n$ , which is related to the rank of the matrix  $\bar{Y}_k' \bar{Y}_k$ .

<sup>1</sup>Which is equivalent to the condition  $E_i \neq 0$  for all  $i = 1, \dots, n$ .

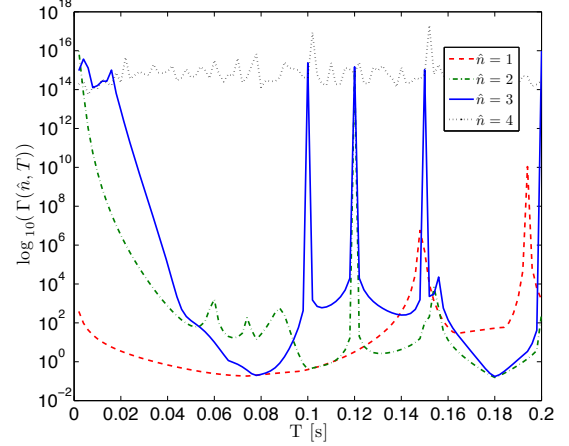


Fig. 1. Dependence of the condition number of  $\bar{Y}_k$  as a function of the sampling time  $T$  and  $\hat{n}$  with the measured signal (18) and  $n = 3$ .

Coherently with this fact, we exploit the dependency on  $\hat{n}$  and  $T$  of the function

$$\Gamma(T, \hat{n}) := |\lambda_{\min}(\bar{Y}_k' \bar{Y}_k)|^{-1},$$

where  $\bar{Y}_k \in \mathbb{R}^{2\hat{n} \times 2\hat{n}}$  and (see (3))  $Y_k = [y(t_k - 2\hat{n}T), \dots, y(t_k - T)]'$ .

*Remark 2:* To retrieve the correct  $n$ , it is also possible to invert the matrix  $\bar{Y}_k$  and obtain  $\hat{a}$  using (10) for different  $n$ , selecting the one which minimizes  $|y(t_k) - \hat{a}Y_k|$ . However, the numerical computation of the minimum eigenvalue of  $\bar{Y}_k' \bar{Y}_k$  more efficient.

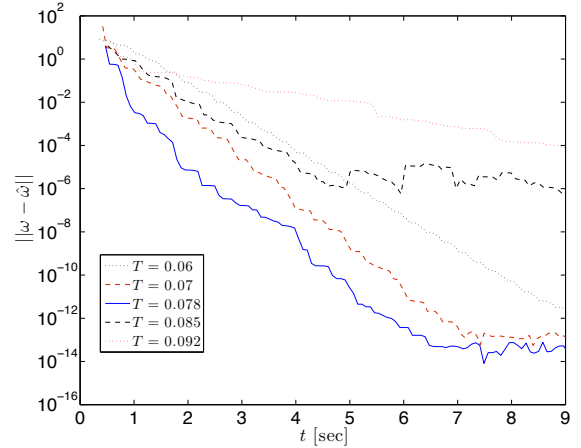


Fig. 2. Simulation result: convergence of the estimation error with different sampling time  $T$ .

An illustration of the function  $\Gamma(T, \hat{n})$  is shown in Fig. 1 with

$$y(t) = \sin(t2\pi/0.7) + \sin(t2\pi/0.3) + \sin(t2\pi/0.2), \quad (18)$$

$$f(\omega) = \begin{bmatrix} -2 \cos(\omega_3 T) - 2 \cos(\omega_2 T) - 2 \cos(\omega_1 T) \\ 3 + 4 \cos(\omega_3 T) \cos(\omega_2 T) + 4 \cos(\omega_3 T) \cos(\omega_1 T) + 4 \cos(\omega_1 T) \cos(\omega_2 T) \\ -4 \cos(\omega_2 T) - 4 \cos(\omega_1 T) - 4 \cos(\omega_3 T) - 8 \cos(\omega_3 T) \cos(\omega_1 T) \cos(\omega_2 T) \end{bmatrix}, \quad (16)$$

$$\nabla f(\omega) = \begin{bmatrix} 2 \sin(\omega_1 T) T & 2 \sin(\omega_2 T) T & 2 \sin(\omega_3 T) T \\ -4 \sin(\omega_1 T) T (\cos(\omega_3 T) + \cos(\omega_2 T)) & -4 \sin(\omega_2 T) T (\cos(\omega_3 T) + \cos(\omega_1 T)) & -4 \sin(\omega_3 T) T (\cos(\omega_2 T) + \cos(\omega_1 T)) \\ 4 \sin(\omega_1 T) T (1 + 2 \cos(\omega_3 T) \cos(\omega_2 T)) & 4 \sin(\omega_2 T) T (1 + 2 \cos(\omega_3 T) \cos(\omega_1 T)) & 4 \sin(\omega_3 T) T (1 + 2 \cos(\omega_1 T) \cos(\omega_2 T)) \end{bmatrix} \quad (17)$$

and  $T_s = 0.002$ . It is evident that for  $\hat{n} = n = 3$  the first peak corresponds to 0.1 that is half of the shorter period 0.2 among the sinusoids composing  $y(t)$ , namely  $0.1 = \pi / \max_i \{\omega_i\}$ . If  $\hat{n} > n$  the value is extremely high denoting  $\text{rank}(\hat{Y}_k) < 2\hat{n}$ . Note as well the high values of  $\Gamma(T, \hat{n})$  for very small  $T$  since the signal changes very little among different samples and the columns of  $\hat{Y}_k$  are “numerically” (bad conditioned) dependent.

From Fig. 1 it should be clear how the function  $\Gamma(T, \hat{n})$  could help to select  $\hat{n}$  and  $T$ . More precisely the value of  $T$  that minimizes  $\Gamma$  before the first spike is encountered can be considered. In this example with the signal (18), once  $\hat{n} = 3$  has been selected, the optimum  $T$  is equal to  $\arg \min_T \{\Gamma(T, \hat{n})\} = 0.078$ . The performances of the estimates provided by  $\mathcal{H}$  using (15) and  $\hat{\omega}^+ = \omega$  in place of  $\hat{a}_c = -\gamma \hat{S}' \zeta e$  and  $\hat{a}_c^+ = \hat{a}_c$  in (14b)-(14c), respectively, are shown in Fig. 2, where the norms of the estimation error  $\|\omega - \hat{\omega}\|$  for different values of  $T \in \{0.06, 0.07, 0.078, 0.085, 0.092\}$  are depicted. To implement (15) we have obtained (16) and (17) using symbolic calculus software, and

$$e = y(t_k) - Y_k' \hat{S} \begin{bmatrix} 1 \\ f(\hat{\omega}) \end{bmatrix}, \quad \hat{S} = \begin{bmatrix} 1 & 0 & 0 & 0 \\ 0 & 1 & 0 & 0 \\ 0 & 0 & 1 & 0 \\ 0 & 0 & 0 & 1 \\ 0 & 0 & 1 & 0 \\ 0 & 1 & 0 & 0 \end{bmatrix}.$$

We also show in Fig. 3 the time evolution of the estimates with  $T = 0.078$  which minimizes the function  $\Gamma(T, \hat{n})$  selecting  $\hat{n} = 3$ ,  $\gamma = 1$ , and  $\hat{\omega}_i(0, 0) = i$  for  $i = 1, 2, 3$ . For numerical reason we have selected  $\gamma = 1$  and let  $\mathcal{H}$  flowing for an equivalent time of 10s among each sampling time  $T$ . The same result can be obtained integrating the flow map for  $T$  seconds, i.e. within the inter-sample time, with  $\gamma = 10/T$ . However, to improve numerical integration it is more convenient to select a smaller  $\gamma$  and a longer “virtual” flowing time between jumps. This can be done online accordingly to the computing power of the hardware implementing  $\mathcal{H}$ .

In the presence of noise it is possible to robustify the results simply increasing the measurements, i.e. the length of  $Y_k$ . An example of the function  $\Gamma(T, \hat{n})$  when the signal (18) is affected by additive uniformly distributed random noise between  $[-0.2, 0.2]$  (equivalently to 20% of the sinusoidal components amplitude) is shown in Fig. 4, where  $\Gamma(T, \hat{n})$  is evaluated using an extra amount of samples, in number of  $w$ , that are stacked at the bottom of  $Y_k \in \mathbb{R}^{(2n+w) \times 2n}$ . Note how the difference of  $\Gamma(T, \hat{n})$  among the correct value

$\hat{n} = 3 = n$  and  $\hat{n} = 4 > n$  is smaller than in Fig. 1.

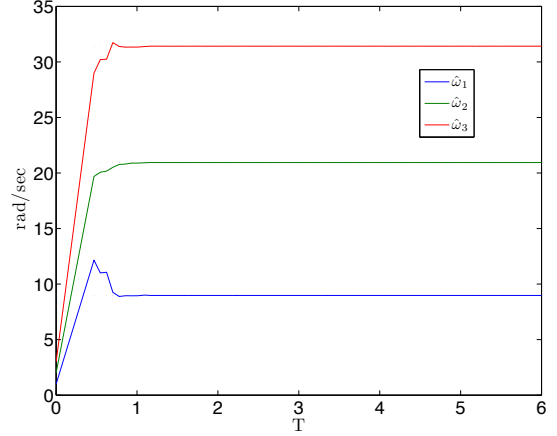


Fig. 3. Estimated angular frequencies when  $\hat{n} = n$ ,  $T = 0.078$ ,  $\gamma = 1$ , and  $\hat{\omega}_i(0, 0) = i$  for  $i = 1, 2, 3$ .

We have discussed how to select  $\hat{n}$  and  $T$  analyzing a window of the past data via the  $\Gamma$  function. We propose now a numerical technique to detect the correct value of  $n$  introducing a  $n$ -dimensional vector  $\mathcal{I}(k)$  whose  $i$ -th components take values in  $\{0, 1, 2\}$ , for different  $j$ ,  $T = jT_s$ , as follows

$$\mathcal{I}_i(j) = \begin{cases} 0 & \text{if } \mathcal{I}_i(j-1) = 0 \wedge g_i(j) > S_a G_{s,i}, \\ 1 & \text{if } (\mathcal{I}_i(j-1) = 1 \wedge g_i(j) < S_b G_{s,i}) \vee \\ & (\mathcal{I}_i(j-1) = 0 \wedge g_i(j) < S_a G_{s,i}) \\ 2 & \text{if } ((\mathcal{I}_i(j-1) = 1 \wedge g_i(j) \geq S_b G_{s,i}) \wedge \\ & \mathcal{I}_{i+1, \dots, N}(j) < 1) \vee \mathcal{I}_i(j-1) = 2 \end{cases} \quad (19)$$

where  $g_i(j) = \Gamma(jT_s, i)$ ,  $G_{s,i} = \Gamma(T_s, i)$ ,  $S_b > S_a > 0$  are thresholds values and  $N$  is the maximum number of frequency of  $y$ . The jump map of the variable  $\mathcal{I}_i$  is such that whenever  $\mathcal{I}_i = 2$  then  $n = i$ . In fact if  $i < n$ , the function  $\Gamma(jT_s, i)$  decreases as  $j$  grows to reach a minimum and then it increases as  $jT_s$  approaches  $\pi/\omega_{\max}$ .

The threshold value  $S_a$  and  $S_b$  have been added to detect that a first minimum has been reached. An example of the relay-like graph of  $\mathcal{I}_i$  is shown in Fig. 5.

Assuming that  $n < N$  and a data buffer  $y_b$  of the past input  $y$  to evaluate  $\hat{Y}_k$  for different  $T$  is properly defined and measured, the algorithm to select  $\hat{n}$  and  $T$  is the following.

#### Algorithm 1

- 1) Select  $N$ ,  $S_a$ ,  $S_b$ . Set  $\hat{n} = 0$ ,  $j = 2$ ,  $\mathcal{I}_i(1) = 0$  and evaluate  $G_{s,i} = \Gamma(T_s, i)$  for  $i = 1, \dots, N$ .

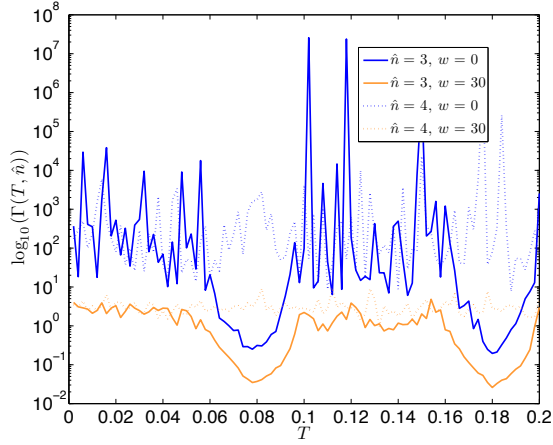


Fig. 4. The function  $\Gamma(T, \hat{n})$  in presence of additive noise on the signal (18) considering extra samples ( $w = 30$ ).

- 2) **While**  $\max_{i=1, \dots, n} \mathcal{I}_i(j) < 2$  **do**  
 Evaluate  $\mathcal{I}_i(j)$  by (19) with  $T = jT_s$  and for  $i = 1, \dots, N$ . Set  $j = j + 1$ .
- 3)  $\hat{n} = \operatorname{argmax}_{i=1, \dots, N} \mathcal{I}_i$ ,  $T = \operatorname{argmin}_{\tau} \Gamma(\tau, \hat{n}) = jT_s$ .

*Remark 3:* The algorithm can be readily extended to the case where  $N$  dynamically grows and the a priori bound  $n < N$  is not known.

To continuously evaluate on-line  $\hat{n}$  and  $T$ , we propose the next algorithm that exploits  $a_c$  in (12) to verify if the  $\omega$  or  $n$  is changed.

#### Algorithm 2

For each new sample:

- if**  $\hat{n} = 0$ : run **Algorithm 1** and evaluate  $a_c$
- else** : if  $|e(t, k)| = |y(t_k) + Y_k' \hat{S}[1, \hat{a}_c(t, k)]'| > S_e \|y(t_k)\|$   
 set  $\hat{n} = 0$  and empty the data buffer  $y_b$ .

The parameters that have to be selected are  $S_a > 0$ ,  $S_b > 0$  such that  $S_a < S_b$ , and  $S_e > 0$ . An example is discussed in Section IV. Note that  $S_e$  limits the number of time the Algorithm 1 is performed.

*Theorem 2:* Let Assumption 1 hold and assume that  $\omega(t)$  and  $n(t)$  are piecewise constant. Perform the **Algorithm 2** to retrieve  $\hat{n}$  and  $T$  at each new sample of  $y$  and, whenever  $\hat{n}(t) > 0$ , evaluate the dynamics (14) of  $\mathcal{H}$  with initial conditions  $\hat{\omega}_i(0)$ ,  $i = 1, \dots, \hat{n}$ , evaluated as the roots of the characteristic polynomial (5) with coefficients yield by (11). Let  $\tilde{a}_c(t, k) := a_c - a(t, k)$ , then whenever  $\omega(t)$  and  $n(t)$  do not change long enough such that  $\hat{n}(t) = n$ ,  $t \in [t_k, t_{k+1}]$ , it holds

$$\|\tilde{a}_c(t, k)\| \leq \|\tilde{a}_c(t_{\bar{k}}, \bar{k})\| e^{\sigma(t)(t-t_{\bar{k}}-4nT(t_k))}, \quad (20)$$

with  $\sigma(t) := \lambda_{\min}(\bar{Y}'_k \bar{Y}_k)$ , and

$$Y_k := [y(t_k - 2nT(t_k)), \dots, y(t_k - T(t_k)), y(t_k)]',$$

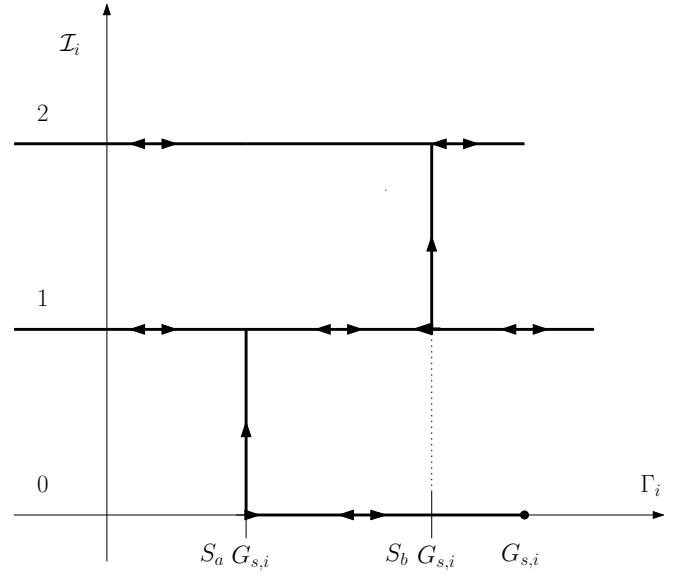


Fig. 5. The graph of  $\mathcal{I}_i$ .

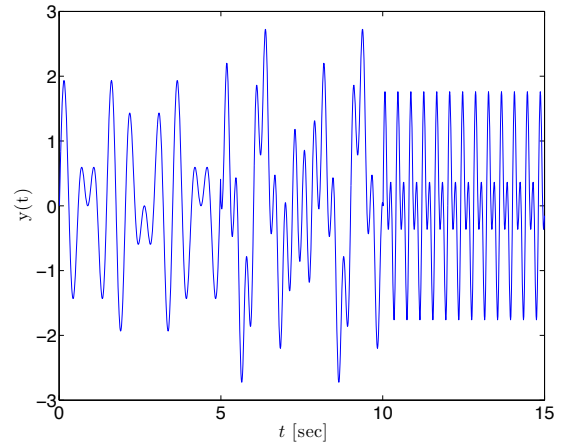


Fig. 6. The signal  $y(t)$  with changing frequencies.

otherwise if  $\hat{n}(t) > 0$ , then

$$|e(t, k)| = |y(t_k) + Y_k' \hat{S}[1, \hat{a}_c(t, k)]'| \leq S_e \|Y_k\|. \quad (21)$$

#### IV. NUMERICAL SIMULATIONS

We show the effectiveness of the observer to retrieve the exact number of frequencies with the signal (see Fig. 6)

$$y(t) = \begin{cases} \sin(2\pi/0.7t) + \sin(2\pi/0.5t) & t \in [0, 5) \\ \sin(2\pi/1.5t) + \sin(2\pi t) + \sin(2\pi/0.3t) & t \in [5, 10) \\ \sin(2\pi/0.4t) + \sin(2\pi/0.2t) & t \geq 10. \end{cases} \quad (22)$$

The observer thresholds have been selected equal to  $[S_a, S_b, S_e] = [0.7, 0.8, 10^{-4}]$ . Note that the selection of these parameters do not depend on the amplitude and the frequency of the sinusoidal terms in (22), but from the signal/noise ratio.

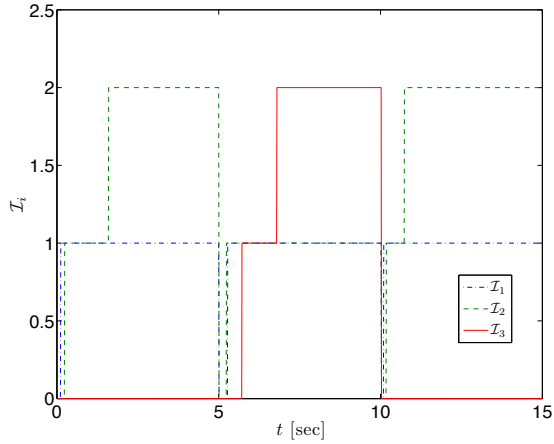


Fig. 7. The graph of  $\mathcal{I}_i$  with the signal (22).

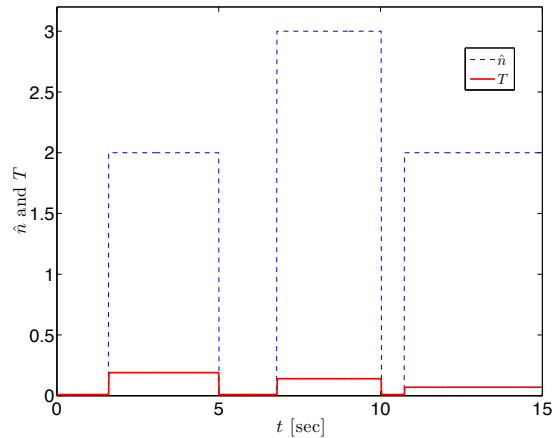


Fig. 8. The estimated number of frequencies and the associated  $T$  with the signal (22).

We also run the simulation example where a uniformly distributed random noise between  $[-0.3, 0.3]$  is added to the signal (22). The estimated frequencies are just like in Fig. 8, however, the observer thresholds have been selected as  $[S_a, S_b, S_e] = [0.3, 0.8, 0.8]$  and the matrix  $Y_k \in \mathbb{R}^{2n+40}$  has been enlarged to contain 40 extra samples. Note the  $S_e$  (see the **Algorithm 2**) need to be increased with measurement noise.

## V. CONCLUSIONS

We have proposed a numeric procedure to estimate the number of frequencies  $n$  of the signal (1) and to select the re-sampling time  $T$  that improves the performances of the hybrid observer for multiple frequencies estimation in [1]. The proposed method has been tailored for numerical implementation. We have given theoretical and numerical

evidence that the function  $\Gamma(T, \hat{n})$  can be exploited to retrieve  $n$  and select  $T$ . Numerical simulations have been performed to show the effectiveness of the approach, shown to be robust with respect to measurement noise.

## REFERENCES

- [1] D. Carnevale, S. Galeani, and A. Astolfi, "Hybrid observer for multi-frequency signals," in *IFAC Workshop Adaptation and Learning in Control and Signal Processing (ALCOSP)*, Elsevier, Ed., vol. 10, Antalya, 2010.
- [2] S. M. Kay and S. L. Marple, "Spectrum analysis – a modern perspective," *Proc. IEEE*, vol. 69, no. 11, pp. 1380–1419, 1981.
- [3] P. Regalia, "An improved lattice-based adaptive iir notch filter," *IEEE Trans. Signal Processing*, vol. 39, pp. 2124–2128, Sept. 1991.
- [4] S. Bittanti and S. Savaresi, "On the parameterization and design of an extended kalman filter frequency tracker," *IEEE Trans. Automat. Contr.*, vol. 45, no. 9, pp. 1718–1715, 2000.
- [5] L. Hsu, R. Ortega, and G. Damm, "A globally convergent frequency estimator," *IEEE Trans. Autom. Contr.*, vol. 44, no. 4, pp. 698–713, 1999.
- [6] S. Sastry and M. Bodson, *Adaptive Control: Stability, Convergence and Robustness*, U. S. River, Ed. NJ, Prentice–Hall, 1989.
- [7] X. Xia, "Global frequency estimation using adaptive identifiers," *IEEE Trans. Autom. Contr.*, vol. 47, no. 7, pp. 1188–1191, 2002.
- [8] G. Obregon-Pulido, B. Castillo-Toledo, and A. Loukianov, "A globally convergent estimator for n-frequencies," *IEEE Trans. Autom. Contr.*, vol. 47, no. 5, pp. 857–863, 2002.
- [9] R. Marino and P. Tomei, "Global estimation of n unknown frequencies," *IEEE Trans. Autom. Contr.*, vol. 47, no. 8, pp. 1324–1328, 2002.
- [10] D. Carnevale and A. Astolfi, "A minimal dimension observer for global frequency estimation," in *Proc. IEEE American Control Conference, Seattle, Washington*, 2008, pp. 5269–5274.
- [11] R. Marino and G. L. Santosuosso, "Regulation of linear systems with unknown exosystems of uncertain order," *IEEE Trans. Automatic Control*, vol. 52, no. 2, pp. 352–359, feb. 2007.
- [12] J. Hoagg, M. Santillo, and D. Bernstein, "Discrete-time adaptive command following and disturbance rejection with unknown exogenous dynamics," *Automatic Control, IEEE Transactions on*, vol. 53, no. 4, pp. 912–928, may 2008.
- [13] S. Galeani, D. Carnevale, and A. Astolfi, "An adaptive hybrid robust regulator," in *IEEE Conf. Decision and Contr.*, 2011, submitted.
- [14] R. Goebel, R. Sanfelice, and A. R. Teel, "Hybrid dynamical systems," *IEEE Control Systems Magazine*, vol. 29, pp. 28–93, 2009.